Journal of Molecular Catalysis B: Enzymatic 104 (2014) 48–55

Contents lists available at ScienceDirect

Journal of Molecular Catalysis B: Enzymatic

journal homepage: www.elsevier.com/locate/molcatb

Immobilization of endo-inulinase on non-porous amino functionalized silica nanoparticles

Mahsan Karimi[a,b], Isthier Chaudhury[c], Cheng Jianjun[c], Mohammad Safari[b], Rohollah Sadeghi[a,b,1], Mehran Habibi-Rezaei[d,e,*], Jozef Kokini[a,**]

[a] Department of Food Science and Human Nutrition, College of Agriculture, Consumer and Environmental Sciences, University of Illinois, Urbana, IL, USA
[b] Department of Food Science and Engineering, Faculty of Agricultural Engineering and Technology, University of Tehran, Karaj, Iran
[c] Department of Materials Science and Engineering, College of Engineering, University of Illinois, Urbana, IL, USA
[d] School of Biology, College of Science, University of Tehran, Tehran, Iran
[e] Nano-Biomedicine Center of Excellence, Nanoscience and Nanotechnology Research Center, University of Tehran, Tehran, Iran

ARTICLE INFO

Article history:
Received 24 October 2013
Received in revised form 14 January 2014
Accepted 30 January 2014
Available online 4 March 2014

Keywords:
Inulinase
Non-covalent adsorption
Covalent attachment
Cross linking immobilization
Silica nanoparticles

ABSTRACT

Endo-inulinase (EC 3.2.1.7) from *Aspergillus niger* as a key enzyme in catalytic hydrolysis of inulin and production of high fructose syrup (HFS) was immobilized on aminated non-porous silica nanoparticles (NPs) with particle sizes of 50, 100 and 200 nm. These particles were synthesized and Fourier transform infrared spectroscopy (FTIR), scanning electron microscopy (SEM) and dynamic light scattering (DLS) were used to characterize them. The immobilization was carried out by three methods including non-covalent adsorption (nC), covalent attachment (C) and cross linking (CL) using glutaraldehyde (GA). The immobilized enzymes were functionally characterized in terms of their optimum temperature, thermal stability and reusability. Results revealed that 50 nm silica NPs had the highest efficiency in immobilizing inulinase. As a result, thermal stability was improved and the activity was counter correlated with the particle size in immobilization products. Results of thermodynamic analysis showed that E_{in}, ΔH° and ΔG° for all the immobilized forms were higher than that of the free enzyme suggesting that a higher level of energy is required to denature the immobilized enzyme, making the immobilized enzymes substantially more stable than the free enzyme. Results of the operational stability analysis showed that the enzyme immobilized via non-covalent adsorption, covalent attachment and cross linking preserved 56.45, 65.45 and 80.75% of their initial activities after 7 cycles of hydrolysis, supporting the fact that the cross linking method is the superior method. The optimum temperature was shifted from 50 °C for the free and non-covalent products to far higher temperatures for the covalent and the cross linking products. As a result, immobilization and brightly cross linking strategy brings about thermal stability and elevates the optimum temperature which is necessary for endoinulinase application in industry.

1. Introduction

Inulinase belongs to glycoside hydrolase family GH32 (1-β-D-fructan hydrolase, EC 3.2.1.7). They have been widely applied as biocatalysts to hydrolyze inulin to produce primarily fructose with a small amount of glucose [1]. Inulin is a reserve carbohydrate in the roots and tubers of Jerusalem artichoke, chicory, dahlia and other sources and is industrially important to produce high fructose syrup (HFS) [2]. It consists of linear chains of D-fructose with a glucose terminal group at the reducing end [3].

Immobilization of enzymes facilitates recovery of products, enables the reutilization of the high value enzyme and makes industrial processing economical [4–6]. Various immobilization strategies have been reported which could be classified as non-covalent (adsorption) and covalent immobilization methods. Covalent immobilization is usually preferred if it retains the enzyme activity by avoiding enzyme leakage from the support. Nanoparticles (NPs) have been widely applied to host enzymes because they offer high surface area to volume ratio which results in higher enzyme loading with low mass transfer resistance [7].

* Corresponding author at: School of Biology, College of Science, University of Tehran, Tehran, Iran. Tel.: +98 21 61113214; fax: +98 21 66492992.
** Corresponding author. Tel.: +1 217 244 4498.
E-mail addresses: karimimahsun@gmail.com (M. Karimi), Chaudhu2@illinois.edu (I. Chaudhury), jianjunc@illinois.edu (C. Jianjun), msafari@ut.ac.ir (M. Safari), sadeghi_r@yahoo.com (R. Sadeghi), mhabibi@khayam.ut.ac.ir (M. Habibi-Rezaei), kokini@illinois.edu, jkokini51@gmail.com (J. Kokini).
[1] He particpated in this research while he was on leave at the University of Illinois during a one year sabbatical from Tehran University.

http://dx.doi.org/10.1016/j.molcatb.2014.01.025
1381-1177/

Glutaraldehyde (GA) activation of amino-functionalized supporting agents is one of the most efficient enzyme immobilization strategies [8] which acts as a cross linker to attach the enzyme to the support by forming Schiff bases [8–10]. In this study we applied noncovalent, covalent and cross linking strategies to prepare, then compare the immobilization products. Non-covalent adsorption of inulinase occurs through interactions like hydrogen bonds, electrostatic forces and hydrophobic interactions [11]. Reducing the size of the supporting material, provides greater surface to volume ratio of particles, and results in much greater loading of the enzyme per unit mass of the support [12]. Among them, nano-sized silica particles have received much attention as efficient host materials for enzyme immobilization [13,14] owing to their uniform shape, chemical and mechanical stabilities, small diffusion limitation and their small size, high surface to volume ratio which increases the enzyme loading per unit mass of the support.

In cross linking immobilization, first layer of enzyme is covalently attached to the supporting agent that could be aggregated in the presence of excess free enzyme using GA treatment. These cross linked immobilized-enzyme aggregates could overcome the limitation in maximum enzyme loading capacity in covalent attachment which is due to the mono layer coverage of the enzyme molecules on the supporting agent and at the same time, could improve the enzyme activity and stability. Kim et al. developed a unique approach for the fabrication of enzyme aggregate coatings on the surfaces of electrospun polymer nanofibers. They coated α-chymotrypsin on nanofiber electrospun and showed that the initial activity of α-chymotrypsin-aggregate-coated nanofibers was nine times higher than nanofibers with just a layer of covalently attached α-chymotrypsin molecules [15].

Kim et al. developed a biocatalytic system using polymer nanofibers coated with trypsin aggregates. First, an initial layer of trypsin covalently attached to the polymer nanofibers, then more trypsin molecules cross linked to the first layer using GA treatment. This process resulted in an increase in trypsin activity compared to covalently attached trypsin which retained a high level of activity after a year of repeated recycling [16].

In this paper, silica NPs with particle sizes of 50, 100 and 200 nm were synthesized and used for immobilization of inulinase by three methods then, comparisons were made to find the best immobilization method to produce HFS.

2. Materials and methods

2.1. Materials

Sodium potassium tartrate, 3,5-dinitrosalicylic acid (DNS), endo-inulinase (EC 3.2.1.7) from *Aspergillus niger*, glutaraldehyde, tetraethylorthosilicate (TEOS), 3-aminopropyltriethoxysilane (APTS) and potassium bromide were from Sigma Chemical Company (St. Louis, MO, USA). Ammonium hydroxide solution and methanol were obtained from Fisher Scientific. Inulin (from chicory) was received from MP Bio-Medicals, LLC Company (Santa Ana, USA). All other chemicals were of analytical grade. Milli-Q water was used in all the experiments.

2.2. Methods

2.2.1. Preparation and characterization of the nonporous silica materials

Uniform silica NPs with controlled sizes of 50, 100 and 200 nm were synthesized in a reaction mixture of Milli-Q water, methanol, ammonium hydroxide (28–30%) to which, 62.5 μl TEOS, was quickly added while stirring (~400 rpm) then left gently under stirring (100 rpm) overnight at room temperature. Size and morphology of the particles were examined using scanning electron microscopy (SEM) (Hitachi S-4700, Japan, Tokyo) at a voltage of 20.0 kV after coating the samples with a thin layer of Au–Pd by magnetron sputtering. Particle size and distribution were measured using dynamic light scattering (DLS) (Brookhaven Instruments Co., USA).

Amino functionalizing of the surface of silica NPs was achieved through introducing the amino groups on the silanols of the silica NPs followed by adding 4 μl APTS and 1 μl TEOS to the reaction mixture while stirring overnight. NPs were then centrifuged (20,000 × *g*, 10 min) and washed twice with 1 ml of anhydrous ethanol and centrifuged (20,000 × *g*, 10 min), then washed twice with 1 ml of Milli-Q water and centrifuged (20,000 × *g*, 10 min) and finally dispersed in 1 ml of Milli-Q water. To prepare 50 nm NPs, 1 ml methanol, 360 μl Milli-Q water and 90 μl ammonium hydroxide was used while for 100 nm NPs: 1 ml methanol, 360 μl Milli-Q water and 120 μl ammonium hydroxide was used and for 200 nm NPs: 1 ml methanol, 270 μl Milli-Q water and 240 μl ammonium hydroxide was used. The whole procedure was scaled up to 5× [17,18]. To modify the primary amino groups of the supporting agents with GA molecules, 10 mg of amino-functionalized silica NPs was incubated with 100 μl of 1% (v:v) GA solution in 50 mM sodium acetate buffer at room temperature under constant stirring for 2 h. Samples were then washed with 50 mM sodium acetate buffer at pH 5.4 and centrifuged (20,000 × *g*, 10 min) to remove excess of GA [11,19,20]. Fourier transform infrared spectroscopy (FTIR)confirmed the amine and the amine-aldehyde functionalization and also inulinase immobilization on the silica NPs using Perkin Elmer LS 55 (Perkin Elmer, Inc., USA) at 4 cm^{-1} resolution in the range of 500–4000 cm^{-1} [11].

2.2.2. Immobilization of enzyme on silica NPs

Three kinds of enzyme immobilization procedures were used to bind inulinase to 50, 100 and 200 nm silica NPs. These are noncovalent adsorption of the enzyme on the surface of non-porous silica NPs, covalent attachment using GA as a cross linking agent and cross linking strategy in which GA is applied in two steps which could result in a higher concentration of enzyme aggregates. First, inulinase was exposed to the aldehyde groups of GA activated amino functionalized silica NPs to form covalent linkages which could act as an anchor for the enzyme aggregates that are cross linked by exposing inulinase to the cross linker that added at the second step.

For non-covalent adsorption, an enzyme solution (100 μl) at 2.5 mg ml^{-1} in 50 mM sodium acetate buffer at pH 5.4 was added to 10 mg of the amino-functionalized silica NPs and stirred for 24 h at 4 °C [10]. The covalent immobilization was performed by mixing 10 mg of GA-activated amino-functionalized silica NPs and 100 μl of enzyme solution at the same concentration and stirring for 24 h at 4 °C. In enzyme cross linking strategy, covalently immobilized preparation was prepared as previously described then, 100 μl of 0.2% (v:v) GA in 50 mM sodium acetate buffer at pH 5.4 was introduced into the mixture and stirred continuously for 10 h at 4 °C [21]. Inulinase-loaded amino-functionalized particles were then recovered by centrifugation (20,000 × *g*, 10 min).

In order to remove trapped non-bound enzymes, the products obtained by centrifugation were rinsed three times with 50 mM sodium acetate buffer solution in each of the applied strategies. The buffer solution for the rinse was collected to determine the loading of inulinase molecules on the supporting agents [22,23]. To verify the covalent bonds as the main attaching forces between the enzyme and the supporting agents, the enzyme loaded particles with different methods of immobilization were incubated with 1 M NaCl and the leakage of an enzyme in the presence of NaCl was evaluated by measuring the activity of the supernatants pertained to each of the inulinase loaded particles [20].

The mass ratio of immobilized inulinase on the particles represents the enzyme loading capacity (ELC) [9]. However, ELC of inulinase can be defined in two ways; as the units of enzyme and mg of protein loaded per gram of the supporting agents.

2.2.3. Protein content and inulinase activity assays

Protein was determined according to Bradford's method [24] using a Tecan spectrophotometer (infinite M 200, Tecan, Inc., USA). The amount of bound protein was determined indirectly by subtracting the amount of protein introduced into the supporting agents and the protein recovered in the supernatant and washing solutions [25].The activities of free and immobilized inulinases were determined by dinitrosalicylic acid (DNS) method [26]. Briefly, 10 mg of inulinase loaded NPs were incubated with 400 μl of 50 mM sodium acetate buffer at pH 5.4 containing 0.2% inulin. The cocktail was hydrolyzed for 30 min in a water bath shaker at 45 °C. Then the cocktail was centrifuged (20,000 × *g*, 10 min) and the reaction was stopped by adding 400 μl of DNS reagent. The activity of the immobilized inulinase was determined by reading the absorbance intensity at 575 nm using Tecan spectrophotometer (infinite M200, Tecan, Inc., USA) against the blank. One inulinase unit (1 U) is defined as the amount of enzyme required to produce 1 μmol fructose per minute under the assay conditions.

2.2.4. Characterization of immobilization products

The optimum temperatures of the free and immobilized inulinases were determined in the temperature range from 30 to 70 °C. Moreover, Arrhenius plot (regression of natural logarithm of activity versus the reciprocal of absolute temperature) was plotted for each preparation and the activation energy (E_a) or the minimum energy required to start a chemical reaction at each temperature (kJ mol^{-1}) was calculated from the slopes knowing that the activation energy of the catalysis is the function of multiplying the slope and gas constant (R = 8.3145 J mol^{-1} K^{-1}). Thermal stability of the free and immobilized preparations of the inulinase at 50, 60 and 65 °C were also determined [27,28]. Free and immobilized enzymes were incubated and samples were withdrawn at appropriate intervals up to 150 min and assayed in 0.2% inulin at 45 °C. The relative activity is defined as the ratio of the residual activity to the initial activity [9].

Thermal inactivation kinetics of inulinase was assumed to follow a first order kinetics model (Eq. (1)) and the thermal inactivation rate constant (k_{in}) (min^{-1}) was determined as the slope of the linear regression of $\ln(A_t/A_0)$ versus time at constant temperature, whereas the decimal reduction time (D value) (min) was determined from a linear regression analysis of $\log(A_t/A_0)$ versus time at constant temperature. D value is defined as the time required at a certain temperature to lose 90% of the enzyme activity (Eq. (2)) or time required to pre-incubate the enzyme at a given temperature to maintain 10% of the residual activity [29]. Moreover, the half-life of endo-inulinase ($t_{1/2}$, min) or the time required for fifty percent activity loss was determined (Eq. (3)):

$$\ln\frac{A}{A_0} = -k_{in}^{t} \tag{1}$$

$$\log\frac{A_t}{A_0} = -\frac{t}{D} \tag{2}$$

$$t_{1/2} = \frac{\ln 2}{k_{in}} \tag{3}$$

where A_0 is inulinase activity before incubation, A_t is inulinase activity after incubation at the temperature of interest and t is the incubation time.

The Arrhenius equation (Eq. (4)) was used to determine the energy barrier (E_{in}) for inulinase thermal inactivation (J mol^{-1}) pertaining to the free and immobilized inulinases [29]:

$$\ln k_{in} = \frac{-E}{RT} + \ln c \tag{4}$$

The change in enthalpy (ΔH, J mol^{-1}) for inulinase thermal inactivation was determined using Eq. (5) [23]:

$$\Delta H^{\circ} = E_{in} - Rt \tag{5}$$

The free energy (ΔG, J mol^{-1}) and entropy (ΔS°, J mol^{-1} K^{-1}) for the thermal inactivation of inulinase were determined using Eqs. (6) and (7) [29–31]:

$$\Delta G^{\circ} = -RT\ln\left(\frac{K_{in}.h}{k_b.T}\right) \tag{6}$$

$$\Delta S^{\circ} = \frac{\Delta H^{\circ} - \Delta G^{\circ}}{T} \tag{7}$$

where T is the absolute temperature (K), R is the gas constant (8.314 J mol^{-1} K^{-1}), h is the Planck's constant (11.04 × 10^{-36} J min), k_B is the Boltzmann constant (1.38 × 10^{-23} J K^{-1}) and k_{in} is the inactivation rate constant (min^{-1}).

2.2.5. Reusability study

Reusability of the immobilized inulinase on amino-functionalized silica NPs was estimated by incubating 10 mg of inulinase loaded NPs with 400 μl of 50 mM sodium acetate buffer at pH 5.4 containing 0.2% inulin and hydrolyzing the cocktail for 30 min in a water bath shaker at 45 °C, then centrifuging the cocktail (20,000 × *g*, 10 min) and stopping the reaction by adding 400 μl of DNS reagent and finally reading the absorbance intensity at 575 nm against the blank. After each cycle, enzyme loaded particles were washed with sodium acetate buffer and re-introduced into a fresh reaction medium (400 μl of 50 mM sodium acetate buffer at pH 5.4 containing 0.2% inulin) for another assay run and this procedure was repeated 7 cycles [27,32]. Relative activity was expressed as the ratio of the residual activity to the initial activity [9].

3. Results and discussion

Nanoparticles were synthesized, then analyzed using DLS and observed using SEM. Sizes were determined as 56 ± 0.5 nm, 107.5 ± 0.7 nm and 212 ± 0.85 nm representing 50, 100 and 200 nm silica NPs. Also silica NPs before and after surface modification were characterized using FTIR. Fig. 1a shows the SEM image of silica NPs with 50, 100 and 200 nm in diameter. Schematic overviews the triple strategies applied for the immobilization of inulinase on aminated silica NPs (Fig. 1b). Inulinase loaded particles incubated with different concentrations of NaCl, then centrifuged and the supernatant was separated and the hydrolytic activity of each supernatant was assayed. The lack of enzyme leakage from the inulinase loaded particles was confirmed by the absence of enzyme activity in the supernatant which signified covalent cross links whereas the case with the complete leakage of the enzyme from inulinase loaded particles to the surrounding medium caused by detaching immobilized inulinase in the presence of NaCl, signified physically adsorbed enzymes on the silica NPs.

Inulinase immobilized on silica NPs via non-covalent, covalent and cross linking methods are compared in Table 1. Immobilization on 50 nm silica NPs results in the highest bound specific activities and loading capacities represented via activity (ALC) or protein (PLC) compared to 100 and 200 nm particles (Fig. 2a and b), most probably due to the increased surface per unit weight of the support [7,33]. These results are consistent with the results reported by Yang et al. [21]. As a result, the counter correlation between size

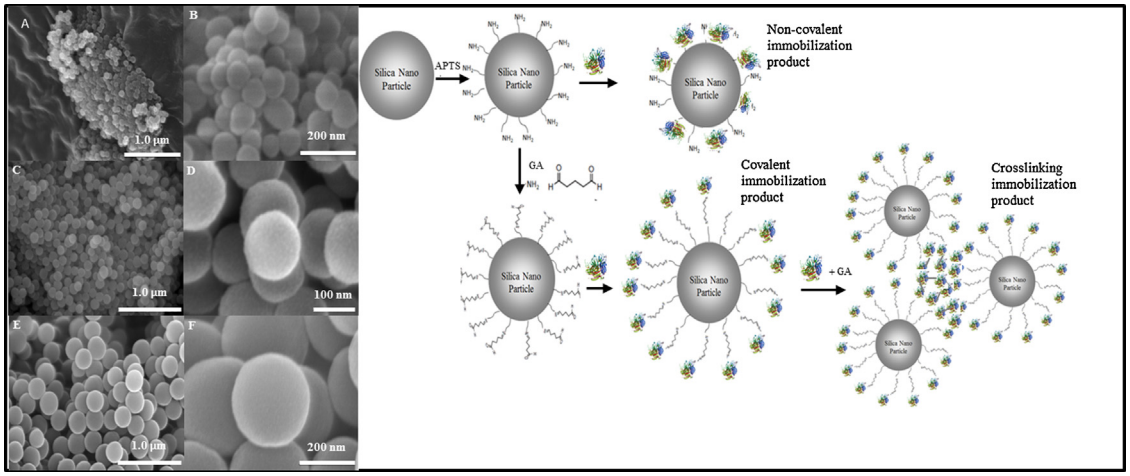

Fig. 1. (Left) SEM images of the silica nano particles of 50 nm (A, B), 100 nm (C, D) and 200 nm (E, F). (Right) Schematic view of the immobilization of inulinase via non-covalent, covalent and cross linking strategies on silica NPs.

of immobilization support and the extent of immobilization seems to be a rule [34]. The specific activity of inulinase is the activity of an enzyme per milligram of the total protein. Moreover, despite the expected higher mass transfer restrictions for the cross linking immobilization product, this immobilization strategy resulted in the higher activity than the covalent and non-covalent methods, which is described by increased enzyme molecules binding per mass of the support without increased conformational disturbance [21]. The latter could be described by more surface accessible lysine constituents in non-catalytic domain (C-domain) than the catalytic domain (N-domain) of inulinase that make it more prone to contribute in GA involved cross linking, which could explain the increase in protein loading capacity and multipoint attachment of the enzyme to the support due to using GA in two steps without binding to the enzyme's active site which could decrease the enzyme activity and this phenomenon seems to overcome the effect of steric hindrances and diffusional limitation [25].

The optimum temperature for non-covalently immobilized endo-inulinase was similar to the optimum temperature of the soluble enzyme at 50 °C, whereas the optimum temperature for covalently and cross link immobilized endo-inulinase were remarkably shifted to higher temperatures due to the increased rigidity of the enzyme structure by immobilization (Fig. 3).

The activation energies of the conversion of inulin for the soluble and three immobilized inulinases were calculated according to the Arrhenius equation and plotted over the appropriate range of the temperatures. The energy barriers for the activity of the free and non-covalently, covalently and cross linked immobilized enzymes on silica NPs were 12.97, 13.47, 4.74 and 6.07 kJ mol^{-1}, respectively. Therefore, the activation energy of the catalysis increased for adsorptive immobilization product whereas; this parameter decreased for glutaraldehyde-involved immobilization products.

Catana et al. reported lower activation energy after inulinase immobilization [35]. Bajpal and Margaritis reported activation energies of 26.6 and 9.5 kJ mol^{-1} for free and gelatin immobilized inulinase [36]. Similarly, Paland Khanum reported decreased E_a upon immobilization of xylanase [37]. Estimating the thermal stability of the biocatalyst is very important. Thermal stability of the

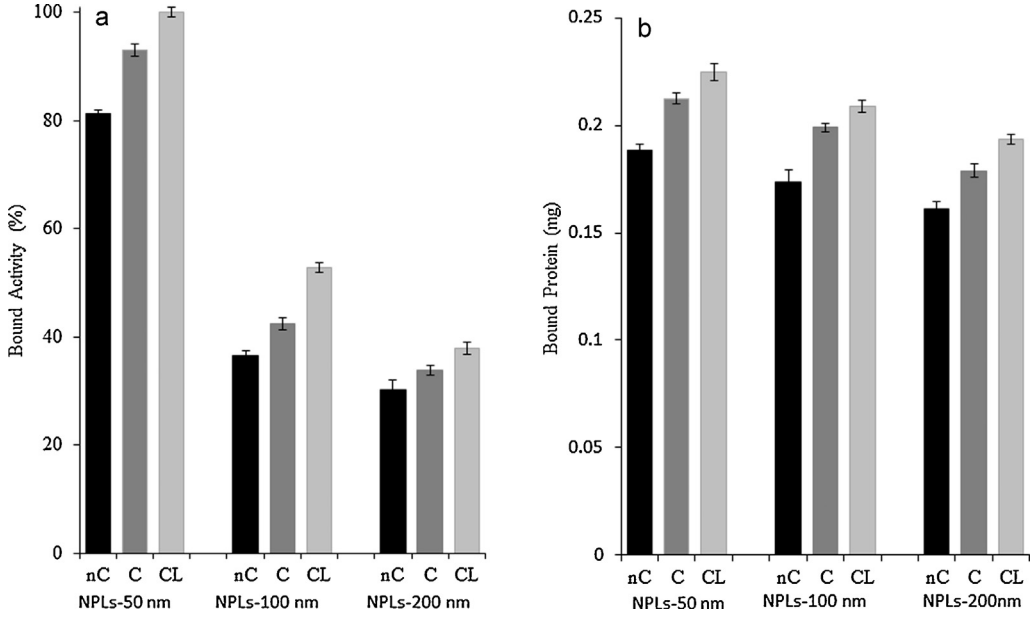

Fig. 2. Bound activity of inulinase immobilized via non-covalent (nC), covalent (C) and cross linking (CL) methods on 10 mg silica NPs with 50, 100 and 200 nm diameter size (a). Bound protein (mg) to 10 mg silica NPs with 50, 100 and 200 nm diameter size after non-covalent (nC), covalent (C) and cross linking (CL) methods (b).

Table 1
Comparing the characteristics of inulinases immobilized via non-covalent, covalent and cross linking immobilization on silica NPs with 50, 100 and 200 nm diameter size.

	nC				C				CL			
	A[a]	SA[b]	ALC[c]	PLC[d]	A[c]	SA[b]	ALC[c]	PLC[d]	A[a]	SA[b]	ALC[c]	PLC[d]
NPs-50 nm	0.458 ± 0.004	2.43 ± 0.02	18.9 ± 0.2	45.8 ± 0.4	0.518 ± 0.006	2.33 ± 0.03	21.3 ± 0.4	51.9 ± 0.6	0.554 ± 0.005	2.47 ± 0.02	22.5 ± 0.5	55.5 ± 0.5
NPs-100 nm	0.229 ± 0.004	1.40 ± 0.02	17.4 ± 0.6	22.9 ± 0.4	0.259 ± 0.006	1.30 ± 0.03	19.9 ± 0.7	25.9 ± 0.6	0.312 ± 0.004	1.57 ± 0.02	20.9 ± 0.2	31.3 ± 0.4
NPs-200 nm	0.197 ± 0.009	1.22 ± 0.06	16.1 ± 0.7	19.7 ± 0.9	0.215 ± 0.009	1.21 ± 0.05	17.9 ± 0.7	21.6 ± 0.9	0.236 ± 0.006	1.22 ± 0.03	19.1 ± 1.1	23.6 ± 0.6

[a] Activity (μmol min^{-1}).
[b] Specific activity (μmol min^{-1} mg^{-1}).
[c] Activity loading capacity (U g^{-1}).
[d] Protein loading capacity (mg g^{-1}).

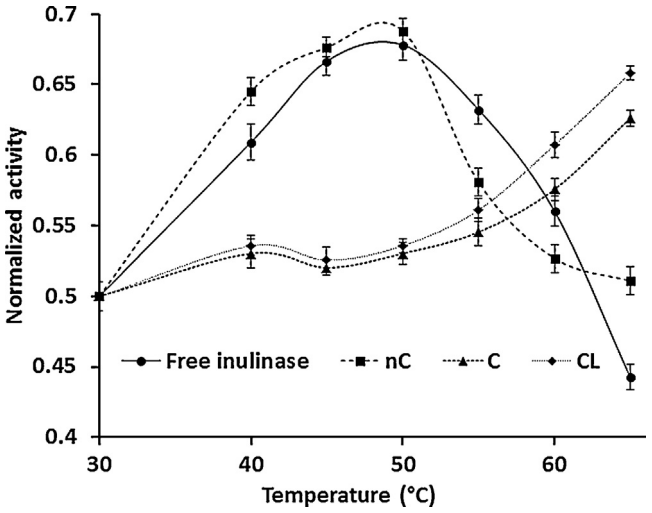

Fig. 3. Optimum temperature of inulinase immobilized non-covalent (nC), covalent (C) and cross linking (CL) methods on silica NPs compared to free inulinase.

free and immobilized inulinase by non-covalent, covalent and cross linking methods at the optimum temperature of catalysis; 50 °C and two higher temperatures; 60 and 65 °C by emphasizing on thermal inactivation kinetics approach for 150 min was studied. As depicted in Fig. 4, thermal resistance was improved after immobilization and amongst the immobilization strategies, cross linking method showed the highest improved stabilization efficiency (73.54, 73.03 and 47.67% residual activity in 50, 60 and 65 °C, respectively). Covalent attachment maintained higher activity (64.49, 41.67 and 42.4% residual activity in 50, 60 and 65 °C, respectively) than the physically attached (55.65, 40.0 and 36.75% residual activity in 50, 60 and 65 °C, respectively) after incubation for 150 min. Yang et al. reported similar results, while Catana et al. [21,35] reported no activity decay for inulinase immobilized onto Amberlite IRC 50 after 1 h of incubation at 60 °C. Improvement of the thermal stability after immobilization has also been reported by Hu et al. and Klein et al. who immobilized β-galactosidase on both macro and nano sized chitosan and reported higher thermal stability for all the immobilized enzymes compared to the free enzyme [27,33].

The inactivation kinetics are described using first-order kinetics confirmed by visual inspection of how it fits the model and also by the regression coefficients (0.85–0.99). Then, the inactivation rate constants could be estimated (Table 2) which increased with increasing temperature and it was the least for the enzyme immobilized by cross linking method compared to free enzyme and enzymes immobilized via other applied immobilization strategies at examined temperatures. $t_{1/2}$ values are shown in Fig. 5 for the free and immobilized inulinases as a function of incubation temperature. As expected, $t_{1/2}$ values decreased with increasing the incubation temperature. However, $t_{1/2}$ values of immobilized enzymes were considerably higher than that of the free at the desired incubation temperature. Therefore, the immobilized inulinase was more stable than the free enzyme. Results of $t_{1/2}$ of inulinase immobilized via different methods showed that inulinase immobilized by non-covalent, covalent and cross linking methods were 1.5, 1.8 and 3.3 times bigger than free form at 50 °C and 1.3, 2.2 and 4.5 times bigger than free inulinase at 60 °C and 1.7, 1.9 and 2.3 times bigger than free inulinase at 65 °C, respectively. These results are in agreement with the finding of Catana et al. [35] who reported approximately 6-fold temperature dependent enhancement in the $t_{1/2}$ of the Amberlite-immobilized inulinase compared to the free inulinase. Wu et al. reported $t_{1/2}$ of 5.70 and 14.16 (h^{-1}) for the free and immobilized catalase covalently immobilized on functionalized titania submicrospheres, which reduced by

Table 2
Effect of temperature on the characteristics of inulinases immobilized via noncovalent, covalent and cross linking immobilization compared to free inulinase.

	50 (°C)			60 (°C)			65 (°C)		
	k_{in} ($\times 10^{-3}$ min^{-1})	$t_{1/2}$ (min)	D (min)	k_{in} ($\times 10^{-3}$ min^{-1})	$t_{1/2}$ (min)	D (min)	k_{in} ($\times 10^{-3}$ min^{-1})	$t_{1/2}$ (min)	D (min)
Free	6	115.52	384.61	8.9	77.88	256.41	11	63.013	208.33
nC	4	173.29	588.24	7.1	97.63	322.58	6.3	110.02	370.37
C	3.4	203.87	666.67	4.1	169.06	555.56	5.9	117.48	384.62
CL	1.8	385.08	1250	2	346.57	833.33	4.8	144.40	476.19

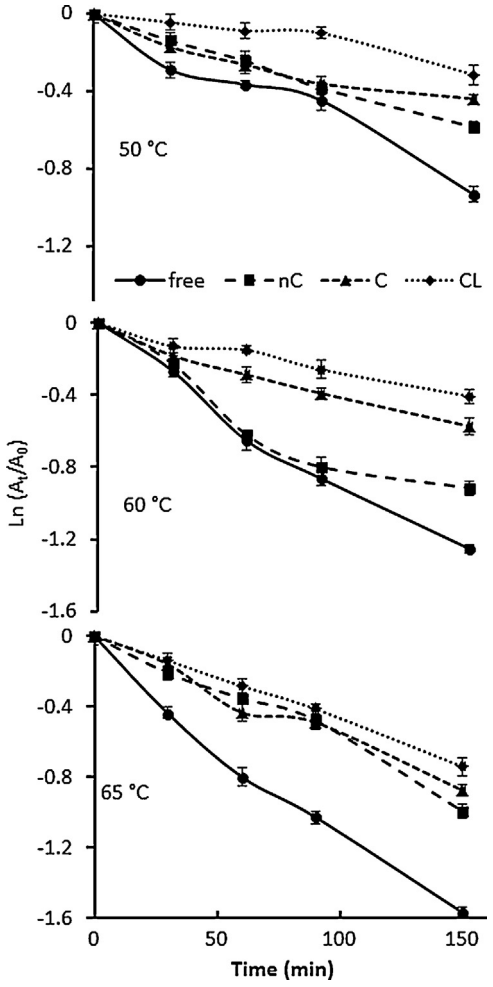

Fig. 4. Thermal stability of inulinase immobilized via inulinase immobilized non-covalent (nC), covalent (C) and cross linking (CL) methods on silica NPs at temperatures of 50, 60 and 65 °C.

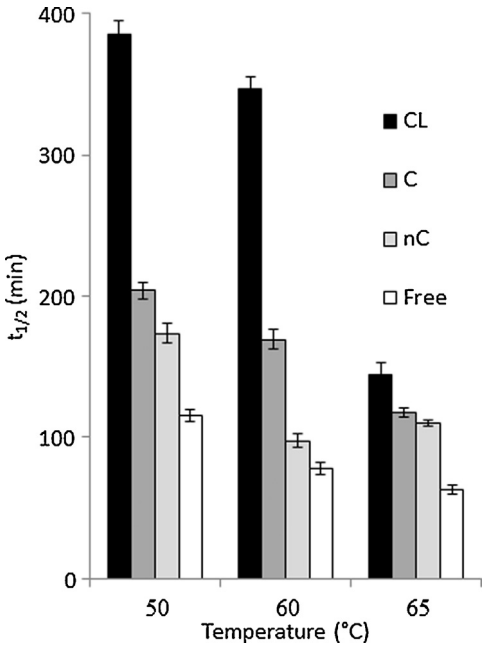

Fig. 5. Half-life of the inulinase immobilized via non-covalent (nC), covalent (C) and cross linking (CL) methods on silica NPs at temperatures of 50, 60 and 65 °C.

increasing temperature [23]. As expected, the time required to achieve 90% activity loss which is represented by D value decreased with increasing temperature and increased after immobilization. The immobilization product of the cross linking method showed the highest D value amongst the next two immobilization products at 1250, 833.33 and 476.19 min at 50, 60 and 65 °C, respectively (Table 2).

The energy barriers of the thermal inactivation (E_{in}) were calculated for the free and immobilized preparations. Resulted E_{in} corresponding to the immobilization products were higher than that that of the free enzyme which confirms the stabilization of inulinase through immobilization, especially in the case of using cross linking strategy. Thermodynamic parameters (ΔH°, ΔG° and ΔS°) for the free and immobilized inulinases were estimated and the results are summarized in Table 3. ΔH° or the heat required to inactivate the enzyme showed a decreasing trend with increasing in temperature at 50–65 °C (Table 3), which reveals less energy is required to inactivate the enzyme at higher temperatures [23,29,38]. As depicted, ΔH° was higher in the immobilized forms compared to the free inulinase and, immobilization product of the cross linking method had the highest values among the immobilized forms indicating that the enzyme undergoes a considerable conformational change during inactivation [39] thus the highest thermal stability was observed in this product.

The free energy for the thermal inactivation; ΔG°, represents the extent of spontaneity of the enzyme inactivation that are higher than the ΔH° values due to the negative entropic contribution to the inactivation processes [40]. The estimated ΔG° values of the free, non-covalent and covalent immobilization products of one-liners increased with increase in temperature. However, in the cross linking products this important parameter increased with the increase in temperature in the initial steps, then decreased.

Moreover, immobilization of inulinase brings about increasing in the free energy for thermal inactivation with positive sign that suggests a greater constraint for inactivation. Therefore, it is noteworthy that the immobilization significantly protects the enzyme from thermal inactivation and as a result cross linking strategy offers again more protection than the next other methods.

When entropy of inactivation (ΔS°) was calculated at each temperature, it resulted in negative values, which indicates that there are significant processes of compaction/aggregation [31,36,39]. We have observed a decreasing ΔH° and negative ΔS° with an increase in the temperature that has also been observed by Rajoka and Riaz [41]. Considering the thermodynamic results presented in Table 3, and correlation and counter correlation of Gibbs free energy of

Table 3
Effect of temperature on the thermodynamic parameters of inulinases immobilized via non-covalent, covalent and cross linking immobilization on silica NPs compared to free inulinase.

	E_{in} (kJ mol^{-1})	50 (°C)			60 (°C)			65 (°C)		
		ΔH° (kJ mol^{-1})	ΔG° (kJ mol^{-1})	ΔS° (kJ mol^{-1} K^{-1})	ΔH° (kJ mol^{-1})	ΔG° (kJ mol^{-1})	ΔS° (kJ mol^{-1} K^{-1})	ΔH° (kJ mol^{-1})	ΔG° (kJ mol^{-1})	ΔS° (kJ mol^{-1} K^{-1})
Free	26.45	23.77	104.06	−0.25	23.68	106.28	−0.25	23.64	107.32	−0.25
nC	26.61	23.92	105.15	−0.25	23.84	106.90	−0.25	23.80	108.89	−0.25
C	33.25	30.56	105.59	−0.23	30.48	108.42	−0.23	30.44	109.07	−0.23
CL	57.26	54.57	107.30	−0.16	54.49	110.41	−0.17	54.45	109.59	−0.16

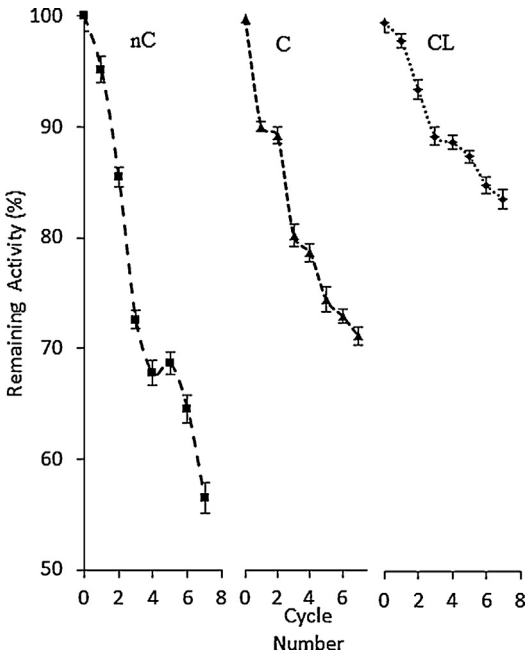

Fig. 6. Reusability of inulinase immobilized via non-covalent (nC), covalent (C) and cross linking (CL) methods on silica NPs incubated with 400 μl of 50 mM sodium acetate buffer at pH 5.4 containing 0.2% inulin for 30 min at 45 °C and this procedure was repeated 7 cycles.

inactivation with enthalpy and entropy, respectively, it can be concluded that the protection of the enzyme from thermal inactivation by immobilization is an enthalpic driven process rather than an entropic driven process.

One of the remarkable features of an immobilized enzyme that makes them different from free enzymes is their reusability (using them repeatedly for several times without much loss of activity) which roots them deeply in the field of biotechnology and make their application economical [11]. The number of successive cycles that an immobilized catalyst can be efficiently reused depends on several factors such as an intrinsic property of the enzyme, employed reaction conditions and the applied method of immobilization.

Our results showed that the enzyme immobilized via non-covalent, covalent and cross linking methods preserve 56.45, 65.45 and 80.75% of their initial activities after 7 cycles of hydrolysis, respectively (Fig. 6).

The loss of activity after some hydrolytic cycles is somewhat because of the inherent inactivation of enzyme as a function of time and more relevantly due to the enzyme leakage which could occur in non-covalent immobilization [32]. Singh et al. reported a 20% loss at the 7th cycle of hydrolysis by immobilizing inulinase on Duolite A568 using GA as a cross linker [42] whereas lipase immobilized by cross linking and covalent attachment preserved 93% and 73% of its original activity after 9 times of recycling, respectively [21]. Xylanase from *Streptomyces olivaceoviridis* E-86 was immobilized on Eudragit S-100 retained 81% of its initial hydrolysis activity after 4 times of recycling [43]. In the other work, xylanase from *Aspergillus niger* was covalently immobilized on the surface of glutaraldehyde–alginate beads could retain more than 85% of its initial activity after 5 times of reusing [29].

4. Conclusion

Inulinase from *Aspergillus niger* was immobilized on 50, 100 and 200 nm GA-activated amino functionalized silica NPs. Immobilization on 50 nm silica NPs offers the highest specific activities

and loading capacities, compared to 100 and 200 nm particles; thus 50 nm supports was chosen as the best support to host the inulinase. Three different immobilization methods including non-covalent, covalent and cross linking were implemented to find the best catalytic properties of enzyme. Inulinase immobilized by cross linking showed both higher activity and stability (thermal and operational) than those of non-covalent and covalent attachment, as it could retain most of its activity after 7 recycles. Hence, we thought that the cross linking method has the potential to stabilize inulinase with higher activity than the other immobilization methods. These results offer great amount of advantages to this immobilized systems for the continuous production of HFS in the industry.

Acknowledgments

This work was conducted at the Department of Food Science and Human Nutrition of the University of Illinois and was supported by USDA Hatch funds. We are grateful to Dr. Bhalerao, Dr. Cheng Jianjun, Dr. Julio Antonio Nieri D Soaresis for their technical assistances. The financial support of the University of Tehran and Iran National Science foundation (INSF) is gratefully acknowledged.

References

[1] W. Lammens, K. Le Roy, L. Schroeven, A. Van Laere, A. Rabijns, W. Van den Ende, J. Exp. Bot. 60 (2009) 727–740.
[2] Z. Chi, Z. Chi, T. Zhang, G. Liu, L. Yue, Appl. Microbiol. Biotechnol. 8 (2009) 211–220.
[3] N. Kaur, A.K. Gupta, J. Biosci. 27 (2002) 703–714.
[4] P. Ye, J. Jiang, Z.K. Xu, Colloids Surf. B 60 (2007) 62–67.
[5] Y.X. Bai, Y.F. Li, Y. Yang, L.X. Yi, J. Biotechnol. 125 (2006) 574–582.
[6] O. Orcaire, P. Buisson, A.C. Pierre, J. Mol. Catal. B: Enzym. 42 (2006) 106–113.
[7] P. Wang, Curr. Opin. Biotechnol. 17 (2006) 574–579.
[8] L. Betancor, F. Lopez-Gallego, A. Hidalgo, N. Alonso-Morales, G. Mateo, R. Fernandez-Lafuente, J.M. Guisan, Enzyme Microb. Technol. 39 (2006) 877–882.
[9] M. Kalantari, M. Kazemeini, F. Tabandeh, A. Arpanaei, J. Mater. Chem. 22 (2012) 8385–8393.
[10] B. Afsahi, A. Kazemi, A. Kheirolomoom, S. Nejati, Sci. Iran 14 (2007) 379–383.
[11] W. Yu, M. Fang, D. Tong, P. Shao, T. Xu, C. Zhou, Biochem. Eng. J. 70 (2013) 97–105.
[12] H. Gustafsson, E.M. Johansson, A. Barrabino, M. Oden, K. Holmberg, Colloids Surf. B 100 (2012) 22–30.
[13] M.E. Mahmoud, A.A. Yakout, H. Abdel-Aal, M.M. Osman, Bioresour. Technol. 134 (2013) 324–330.
[14] A. Ruff, P. Schuler, B. Speiser, J. Solid State Electrochem. 17 (2013) 79–97.
[15] B.C. Kim, S. Nair, J. Kim, J.H. Kwak, J.W. Grate, S.H. Kim, M.B. Gu, Nanotechnology 16 (2005) 382–388.
[16] B.C. Kim, D. Lopez-Ferrer, S.M. Lee, H.K. Ahn, S. Nair, S.H. Kim, B.S. Kim, K. Petritis, D.G. Camp, J.W. Grate, R.D. Smith, Y.M. Koo, M.B. Gu, J. Kim, Proteomics 9 (2009) 1893–1900.
[17] L. Tang, T.M. Fan, L.B. Borst, J. Cheng, ACS Nano 6 (2012) 3954–3966.
[18] L. Tang, N.P. Gabrielson, F.M. Uckun, T.M. Fan, J. Cheng, Mol. Pharm. 10 (2013) 883–892.
[19] A.K. Singh, A.W. Flounders, J.V. Volponi, C.S. Ashley, K. Wally, J.S. Schoeniger, Biosens. Bioelectron. 14 (1999) 703–713.
[20] F. Lopez-Gallego, L. Betancor, C. Mateo, A. Hidalgo, N. Alonso-Morales, G. Dellamora-Ortiz, J.M. Guisan, R. Fernandez-Lafuente, J. Biotechnol. 119 (2005) 70–75.
[21] G. Yang, J. Wu, G. Xu, L. Yang, Colloids Surf. B 78 (2010) 351–356.
[22] C. Oh, J.H. Lee, Y.G. Lee, Y.H. Lee, J.W. Kim, H.H. Kang, S.G. Oh, Colloids Surf. B 53 (2006) 225–232.
[23] H. Wu, Y. Liang, J. Shi, X. Wang, D. Yang, Z. Jiang, Mater. Sci. Eng. C 33 (2013) 1438–1445.
[24] M.M. Bradford, Anal. Biochem. 72 (1976) 248–254.
[25] H. Torabizadeh, M. Habibi-Rezaei, M. Safari, A.A. Moosavi-Movahedi, H. Razavi, J. Mol. Catal. B: Enzym. 62 (2010) 257–264.
[26] G. Miller, Anal. Chem. 31 (1959) 426–428.
[27] Y. Hu, S. Tang, L. Jiang, B. Zou, J. Yang, H. Huang, Process Biochem. 47 (2012) 2291–2299.
[28] C. Bernal, L. Sierra, M. Mesa, J. Mol. Catal. B: Enzym. 84 (2012) 166–172.
[29] A. Pal, F. Khanum, Process Biochem. 46 (2011) 1315–1322.
[30] H. Torabizadeh, M. Habibi-Rezaei, M. Safari, A.A. Moosavi-Movahedi, A. Sharifizadeh, H. Azizianand, M. Amanlou, Appl. Biochem. Biotechnol. 165 (2011) 1661–1673.
[31] A. Pal, F. Khanum, J. Biochem. Technol. 2 (2010) 203–209.
[32] R. Reshmi, S. Sugunan, J. Mol. Catal. B: Enzym. 85–86 (2013) 111–118.
[33] M.P. Klein, M.R. Nunes, R.C. Rodrigues, E.V. Benvenutti, T.M.H. Costa, P.F. Hertz, J.L. Ninow, Macromolecules 13 (2012) 2456–2464.
[34] S.C. Tsang, C.H. Yu, X. Gaoand, K. Tam, J. Phys. Chem. B 110 (2006) (1692) 16914–16920.
[35] R. Catana, M. Eloy, J.R. Rocha, B.S. Ferreira, J.M.S. Cabral, P. Fernandes, Food Chem. 101 (2007) 260–266.
[36] P. Bajpal, A. Margaritis, Enzyme Microb. Technol. 7 (1985) 373–376.
[37] A. Pal, F. Khanum, Process Biochem. 46 (2011) 879–887.
[38] H.N. Bhatti, A. Zia, R. Nawaz, M.A. Sheikh, M.H. Rashid, A.M. Khalid, Int. J. Agric. Biol. 7 (2005) 585–587.
[39] E. Marin, L. Sanchez, M.D. Perez, P. Puyol, M. Calvo, J. Food Sci. 68 (2003) 89–93.
[40] A. Tanaka, E. Hoshino, Biochem. J. 364 (2002) 635–639.
[41] M.I. Rajoka, S. Riaz, Electron. J. Biotechnol. 8 (2005) 177–184.
[42] R.S. Singh, R. Dhaliwal, M. Puri, J. Ind. Microbiol. Biotechnol. 34 (2007) 649–655.
[43] Z. Ai, Z. Jiang, L. Li, W. Deng, I. Kusakabe, H. Li, Process Biochem. 40 (2005) 2707–2710.